ORIGINAL ARTICLE
AICHE Journal

Polysorbate identity and quantity dictate the extensional flow properties of protein-excipient solutions

Kathleen T. Lauser[1] | **Amy L. Rueter**[1] | **Michelle A. Calabrese**[1]

[1]Department of Chemical Engineering and Materials Science, University of Minnesota, Minneapolis, Minnesota, 55455

Correspondence
Michelle A. Calabrese, Department of Chemical Engineering and Materials Science, University of Minnesota, Minneapolis, Minnesota, 55455, USA
Email: mcalab@umn.edu

Funding information
National Science Foundation,Grant No. CON-75851, project 00074041

While protein medications are promising for treatment of cancer and autoimmune diseases, challenges persist in terms of development and injection stability of high-concentration formulations. Here, the extensional flow properties of protein-excipient solutions are examined via dripping-onto-substrate (DoS) extensional rheology, using a model ovalbumin protein (OVA) and biocompatible excipients polysorbate 20 (PS20) and 80 (PS80). Despite similar PS structures, differences in extensional flow are observed based on PS identity in two regimes: at moderate total solution concentrations where surface tension differences drive changes in extensional flow behavior, and at small PS:OVA ratios, which impacts the onset of weakly elastic behavior. Undesirable elasticity is observed in ultra-concentrated formulations, independent of PS identity; higher PS contents are required to observe these effects than with analogous polymeric excipient solutions. These studies reveal novel extensional flow behaviors in protein-excipient solutions, and provide a straightforward methodology for assessing the extensional flow stability of new protein-excipient formulations.

KEYWORDS
rheology, *extensional*, polysorbate, protein, excipient

Abbreviations: OVA, ovalbumin; DoS, dripping-onto-substrate extensional rheology; PS80, polysorbate 80; PS20, polysorbate 20.

1 Introduction

Solution-based protein therapeutics, such as monoclonal antibodies (mAbs), are promising for treating a variety of diseases including cancer and COVID-19. These therapeutics, often administered via subcutaneous or intravenous injection, are orders of magnitude larger than small molecule drugs (typically >100 kDa), have complex secondary and tertiary structures, and are difficult to produce. Unsurprisingly, the size and complexity of these cellular therapeutics cause substantial challenges in development, delivery and stability,[1–4] particularly as the solution concentration increases.

New injectable protein therapeutics are largely screened based on their storage stability and shear viscosity, primarily dictated by concentration-dependent protein-protein interactions (PPIs).[5–7] While the stability of protein-excipient formulations at rest is critical for extending shelf life, these metrics are not indicative of stability during injection flows in which proteins experience both shear and extensional forces.[2] These injection flows can accelerate protein aggregation and denaturing – reducing clinical efficiency and antibody response[8] – and their impact on protein dynamics is not well-understood.[4] Further, flow stability depends on the injection forces, which vary based on injection method and needle size.[8,9] The difficulty in measuring flow stability paired with FDA guidelines on injection viscosity and volume has led to therapeutic administration via dilute, low viscosity intravenous injections, which often require treatment at a hospital.[5,7,10,11]

Subcutaneous injections are the most convenient administration route, as they can be self-administered and are minimally invasive;[4] thus delivery via this route has the potential to reduce the burden on the healthcare system.[5,9–11] However, subcutaneous injections typically require small delivery volumes ($\leq$1.5 mL), concentrated formulations ($\geq$100 mg/mL) and small needles, which increase deformation rates and subsequently reduce efficacy.[6,8,11,12] In addition, ultra-high concentration protein formulations, typically defined as having protein contents above 150 mg/mL,[13,14] can lead to high solution viscosities and undesirable viscoelastic behavior.[3,15] These undesirable flow properties are promoted by the crowded solution environment, which enhances protein self-associations and interactions between proteins and other macromolecules in solution. PPIs include long-range repulsive interactions and short-range interactions – such as hydrogen bonding, dipole-dipole interactions, van der Waals attractions, and hydrophobic interactions – which become increasingly important to the viscosity and stability in crowded solution environments where the inter-molecular distance is similar to or smaller than the protein size.[7,11,12]

Adding stabilizing excipients is one route to reduce the shear viscosity and resulting aggregation and loss of function. Given the vast range of PPIs, numerous excipient types including salts, amino acids, sugars, and surfactants are used to stabilize protein therapeutics.[13,14,16,17] Non-ionic surfactant excipients are of particular interest when examining flow stability, as they are commonly used to prevent protein aggregation and denaturing due to agitation or stress induced by processing.[16,18] However, accurate characterization of protein-excipient rheological properties is limited, largely due to measurement challenges. In commercial shear rheometers, the presence of significant air-liquid interfaces and the fairly long measurement time leads to protein adsorption and film formation at these interfaces, which dominates the torque signal and invalidates the measurement.[19–21] As this aggregation and film formation occurs on the order of minutes to hours,[21,22] the rapid timescale of solution extensional rheology measurements allows this challenge to be bypassed.[23,24] However, despite that extensional flows are expected to have a more detrimental impact on protein structure and function than shear flows, the extensional rheology of protein solutions has been sparsely studied because extensional flows in low viscosity macromolecular solutions must often be generated using custom devices.[23,25–29] While these devices can generate extensional flows, many cannot measure rheological properties like extensional viscosity.

Despite limited measurements of accurate protein-excipient rheology, the mechanisms by which nonionic surfactant excipients like polysorbates or poloxamers stabilize protein solutions is well-characterized. Non-

ionic surfactants primarily stabilize proteins by coating air-liquid and solid-liquid interfaces, which not only lowers the interfacial tension and associated interfacial stresses, but also reduces protein surface adsorption and thereby reducing aggregation and denaturing.[16–18] Surfactant addition can also minimize aggregation and unfolding by associating with hydrophobic regions of the protein, thereby improving colloidal stability.[18,30,31] These protein-surfactant interaction mechanisms are concentration-dependent.[16,18] At low concentrations, these surfactants primarily locate at the air-liquid interface, reducing the interfacial tension, and largely avoid interacting with proteins. At higher concentrations, surfactants can interact with the protein surface as the air-liquid interface becomes saturated; in this region, the surface tension decreases nearly linearly with the logarithm of the surfactant concentration.[18,32] At surfactant concentrations above the critical micelle concentration (CMC), micelles can also form in solution and further increases in surfactant concentration have a negligible effect on the solution surface tension[18].

A number of recent studies have demonstrated that concentration-dependent protein-excipient interactions have significant implications for formulating high concentration therapeutics.[13,14,23,33] For example, Rodrigues et al.[13] showed that the optimal excipients for shear viscosity reduction in moderately concentrated monoclonal antibody (mAb) formulations (100 mg/mL) were not predictive of properties in high concentration formulations (≥137 mg/mL). In fact, the worst excipients in the moderately concentrated formulations performed the best in ultra-concentrated mAbs (237 mg/mL)[13]. Whitaker et al.[14] screened 56 excipients across a range of excipient types, noting a dramatic, often exponential increase in solution shear viscosity for mAb solutions with fixed excipient contents between concentrations of 100 and 200 mg/mL mAb. Similar to Rodrigues et al.[13], the authors found that the viscosity at ultra-high concentrations was not well-correlated to the viscosity at 100 mg/mL in many cases, nor the viscosity at 150 mg/mL in several cases. While pharmaceutical producers select excipient concentrations based on the lowest effective stabilizing concentration,[17] Whitaker et al.[14] also found that significantly increasing the excipient concentration (often by an order of magnitude or more) was highly effective in reducing the viscosity of ultra-high concentration mAbs (175 mg/mL) across a range of excipient types, without a detrimental impact on long-term stability. Bhambhani et al.[33] similarly found that high concentrations (≥15%) of several excipient types lead to greater protein conformational stability without detrimental effects in terms of thermal stability. These studies suggest that higher excipient concentrations may be required to adequately stabilize high-concentration protein therapeutics.

While prior studies demonstrate concentration-dependent PPIs and protein-excipient interactions at rest and under shear, recent work suggests that concentration-dependent interactions also result in different behavior in extensional flows. Here, Lauser et al.[23] used dripping-onto-substrate (DoS) extensional rheology to show that interactions between proteins and polymeric excipient P188 in injection-like flows depends on excipient and protein concentration. For example, adding P188 to ovalbumin (OVA) solutions at low or moderate solution concentrations reduced the surface tension, resulting in synergistic flow behavior where the timescale for fluid breakup in OVA/P188 solutions was less than the sum of the two individual components. In this concentration regime, these protein-excipient solutions displayed rapid breakup behavior similar to that of water, indicating good injectability. Unfortunately as the solution concentration increased and the solution surface tension plateaued, the benefits of adding excipient dwindled. In fact, undesirable weakly elastic flow behavior was observed at high concentrations of protein-excipient solutions (300 mg/mL) whereas no elasticity was observed for 300 mg/mL OVA only.[23] This weakly elastic flow behavior results in higher extensional viscosities upon injection, and indicates that the formulation is subjected to large extensional stresses that may detrimentally impact the protein structure and function.

The prior work by Lauser et al.[23] suggests that surfactant excipients added to stabilize proteins at rest or in shear flows can cause detrimental extensional flow properties. However these studies employed P188,

which has a larger molar mass (8.4 kDa) and CMC (~150 mg/mL[34] at RT) relative to many nonionic surfactant excipients. In these studies, solutions of both P188 unimers and P188 unimers coexisting with OVA exhibited elasticity likely due to P188 chain extensibility.[23] Surfactants polysorbate 20 and 80 (PS20 and PS80) are the most commonly employed, FDA-approved surfactant excipients used to stabilize protein medications and vaccines, including for coronavirus.[17,18,35] These two excipients are roughly one order of magnitude smaller in molecular weight than P188 (~1.2 kDa) and have the majority of their molar mass in their identical branched, headgroup; additionally the CMCs for PS20 and PS80 are three to four orders-of-magnitude lower than that of P188.[30,34,36] Thus given the more compact, less extensible structure of polysorbate excipients and their dramatically lower CMC vs. P188, an outstanding question remains as to whether polysorbates impart the same detrimental extensional flow properties in protein-excipient solutions as observed in P188-containing solutions.

While PS20 and PS80 share the same hydrophilic headgroup (SI.1) and have similar molar masses, differences in solution properties and interactions with proteins have been documented,[37] likely due to their differing tail structures: PS20 has a shorter lauric acid tail whereas PS80 instead has a longer, monounsaturated oleic acid tail. The longer hydrocarbon tail in PS80 makes it more hydrophobic, shifting its CMC to lower concentrations relative to PS20 (~0.02 vs. ~0.06 mg/mL at 24 °C, respectively).[18,30,36,38] Above the CMC, PS80 forms slightly larger micelles, with higher aggregation numbers, than PS20.[38–40] These differences in chemical structures and solution behaviors lead to different interactions with proteins. For example, Ruiz-Peña et al.[37] showed that PS20 and PS80 associate with distinct hydrophobic regions of bovine serum albumin (BSA), though PS binding to albumins is low (~1-3 surfactants/protein[31,41]). The authors also showed that the presence of BSA increased the CMC for each polysorbate, but substantially more so for PS80.[37] Additionally, an order-of-magnitude increase in BSA content reduced PS20-BSA interactions by >80%, but had little impact on PS80-BSA interactions.[37] Other studies have shown that added PS addition weakly stabilizes albumins to denaturation, and that PS20-albumin interactions are slightly stronger than those with PS80.[31,41] This difference in interaction strength can be explained by the longer tail and thus larger hydrophobic volume of the PS80 vs. PS20 tail, which leads to distinct – and fewer – binding sites on the protein.[37,41,42] These subtle differences in the concentration-dependent solution properties and interactions of PS20 and PS80 with albumin proteins also suggest that similar differences could be observed in the extensional flow properties.

In this article, ovalbumin solutions in the presence of polysorbates PS20 and PS80 are examined via dripping-onto-substrate extensional rheology to determine how polysorbate quantity and identity impacts protein formulation extensional flow properties. OVA is selected as the model protein to enable direct comparison with prior work on P188 solutions,[23] to compare the stabilization properties of polysorbates in extensional flow differ vs. higher molecular weight, linear surfactants. As prior studies suggest that higher excipient content may be required for adequate stabilization and viscosity reduction in concentrated proteins,[14,33] concentrated protein flow properties are examined with increasing PS20 and PS80 content to determine the PS content required to observe detrimental extensional flow behavior. In addition to PS type and quantity, the protein content is also varied to access a range of macromolecule concentrations in solution, from moderate (100 mg/mL) to ultra-high (300 mg/mL). These measurements of protein extensional flow behaviors in the presence of nonionic surfactant excipients provide a critical dataset for understanding potential detrimental impacts of excipient addition on protein injectability, which can be used to engineer improved excipients that eliminate adverse flow behaviors and improve formulation stability, thereby enabling new and more concentrated injectable therapeutics to be developed.

2 Theory

Capillary-driven thinning and break-up of a liquid bridge is one approach for measuring the extensional rheology

of protein solutions. Here, an unstable liquid bridge is generated between two surfaces, which spontaneously self-thins in the absence of active external forces.[43,44] This liquid bridge is typically generated via plate separation, as done in the commercial capillary breakup extensional rheometry (CaBER) method, or by initially forming a droplet which then slowly contacts a substrate to form the bridge. The latter dripping-onto-substrate (DoS) extensional rheology method[44] enables measurement of lower viscosity solutions than the plate separation method and is ideal for measuring solutions with limited sample volumes such as proteins, as measurements can be performed in $\leq$10 µL.[23,45]

The capillary-driven instability and pinch-off proceeds based on the balance of forces acting on the bridge, including inertial, viscous, elastic, and capillary forces; mathematical descriptions of the thinning behavior based on the relevant forces acting on the bridge can then be used to extract rheological parameters. To select the relevant flow regime, the Ohnesorge number, Oh, quantifies the relative importance of viscous forces to inertial and surface tension forces:

$$Oh = \frac{\eta}{\sqrt{\rho \sigma R_0}} \tag{1}$$

with fluid dynamic viscosity η, density ρ, and surface tension σ; R_0 is the initial radius of the liquid bridge, often taken as the radius of the end plates or nozzle used to generate the bridge. For $Oh \ll 1$, inertial and surface tension forces dominate viscous forces, as is characteristic for low-viscosity fluids like water. The radial decay profiles for low Oh fluids like water that exhibit IC thinning follow a characteristic $t^{2/3}$ scaling[46–48]:

$$\frac{R(t)}{R_0} = \alpha \left(\frac{t_b - t}{t_R} \right)^{\frac{2}{3}} \tag{2}$$

where $R(t)$ is the minimum radius of the liquid bridge at time t, and the Rayleigh time, $t_R = (\rho R_0^3/\sigma)^{1/2}$, is the characteristic timescale for IC thinning phenomena in a fluid of surface tension σ and density ρ. The breakup time, t_b, is the time at which the filament ruptures or breaks up. The prefactor α is treated as a constant, and has been reported experimentally between 0.4 and 1.[43,44,49,50] For IC thinning liquids, the liquid bridge typically assumes a conical shape immediately prior to breakup.

For higher viscosity fluids where $Oh \gg 1$, the liquid undergoes viscocapillary thinning (VC) where viscous forces dominate. In this regime, the power law index associated with thinning increases to unity, where the radial decay can be described as[51]:

$$\frac{R(t)}{R_0} = 0.0709 \left(\frac{\sigma}{\eta R_0} \right) (t_b - t) \tag{3}$$

VC thinning liquids typically present a cylindrical, string-like liquid bridge.[52]

Many complex fluids also exhibit fluid elasticity. Weakly elastic thinning behavior is typically characterized by a slender filament that appears briefly near the end of thinning.[23,53,54] Weakly elastic behavior can be fit using the semi-empirical Anna-McKinley model[53]:

$$\frac{R(t)}{R_0} = Aexp(-Bt) - Ct + D \tag{4}$$

where the coefficient B is a function of the extensional relaxation time, λ_E, as $B \approx 1/3\lambda_E$. The terminal extensional velocity, η_E^∞, can be determined from the coefficient C, where $C \approx \sigma/2\eta_E^\infty R_0$. The coefficient D can be determined from the ratio of C/D and the elastic filament lifetime, t_E, where $D = Ct_E$.[23]

When viscoelastic behavior is more pronounced, the thinning behavior can be described by elastocapillary thinning (EC). EC behavior is often observed in polymer solutions following an initial IC or VC thinning region. In the EC thinning regime, the liquid bridge is cylindrical and thins exponentially with time.[23,44,52] The thinning behavior for EC liquids is described as:

$$\frac{R_{min}(t)}{R_0} \approx \left(\frac{GR_0}{2\sigma} \right)^{1/3} exp\left(\frac{-t}{3\lambda_E} \right) \tag{5}$$

with elastic modulus G, and extensional relaxation time, λ_E.[23,44,52] In the EC thinning regime, macromolecules undergo orientation and conformation changes as well as stretching,[52] which can induce undesirable

stretching, aggregation, and denaturing in protein solutions.[26,27,55]

3 Materials and Methods

3.1 Materials

Ovalbumin (OVA) was obtained from Sigma Aldrich (globular, 42 kDa peptide portion only, 44.3 kDa total, lyophilized powder, >98%) and used as received. Polysorbate 20 (PS20, 1.228 kDa) and polysorbate 80 (PS80, 1.310 kDa) were obtained from Sigma Aldrich and used as received. See SI.1 for the PS chemical structures and the folded OVA structure.

Optically clear polysorbate samples were prepared by dissolving PS20 or PS80 in deionized water. Polysorbate concentration ranged from 1-300 mg/mL for PS20 and 1-250 mg/mL for PS80, concentrations several orders of magnitude above their CMCs at room temperature. Samples were then placed on a refrigerated orbital shaker for a minimum of 12 hours before use to ensure total dissolution. Combined OVA and polysorbate samples were made by dissolving OVA into premade polysorbate solutions. These samples were then placed on a refrigerated orbital shaker for at least 12 hours before measurements were performed.

3.2 Dripping-onto-substrate (DoS) device

Dripping-onto-substrate measurements were performed as previously detailed in Lauser et al.[23] Briefly, a mounted dispensing system is used to create a single hemispherical drop, which makes contact with a glass substrate to create a semi-stable liquid bridge (Figure 1). The substrate surface properties are controlled to ensure similar contact line spreading across comparable solutions. The liquid bridge is illuminated with a light behind a diffusing screen, and the evolution of the liquid bridge radius in time is captured with a high speed camera. As the drop is stationary prior to slowly moving the substrate upwards to form the liquid bridge, the surface tension for each trial can also be determined prior to capillary-driven thinning of the bridge. Fluids measured via DoS in this work reach extension rates of order 10^{-4} (SI.2), in the range for clinically-relevent injection flows.[20]

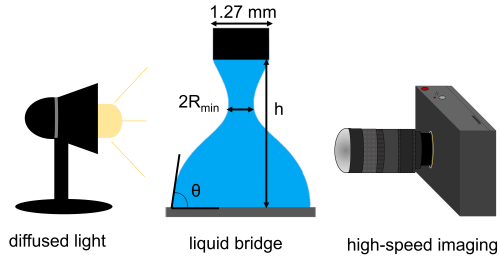

FIGURE 1 Simplified DoS device schematic, comprised of a nozzle that produces a drop which contacts a flat substrate, forming a liquid bridge. The bridge is backlit by diffused light; capillary-driven thinning is captured via high-speed camera.

3.3 Surface tension measurements

The surface tension for each trial was measured using the pendant drop analysis tool in ImageJ,[56] where the drop shape was fit based on the Laplace equation. Images for surface tension measurements were carefully selected to ensure that the drop was stationary (syringe pump off) and had not made contact with the substrate. The validity of this method to determine surface tension was assessed by comparing calculated surface tension values for water (74.1 ± 1.9 mN/m) with the literature value of 72.7 mN/m at 20 °C,[57] as done previously.[23]

3.4 Shear rheology

Shear rheology of polysorbate solutions was measured using an Anton Paar MCR 302 stress-controlled rheometer with a concentric cylinder, 26.7 mm double-gap geometry. Note that the PS-OVA solutions cannot be accurately measured using shear rheology due to the likelihood of interfacial film formation at the air-liquid interface.[20,21] These solutions are low viscosity and are expected to be nearly Newtonian at room temperature; as such, solutions were measured at several shear rates ($\dot{\gamma} \leq 20\ s^{-1}$), with higher shear rates giving an improved torque signal. Reported uncertainties in the viscosity are the standard deviation of multiple measurement points. The viscosities are shear-rate independent within the

measurement uncertainty in this shear rate range, confirming that solutions act nearly Newtonian.

4 Results and Discussion

4.1 Flow behavior of polysorbate solutions

Differences in solution properties that could impact the extensional flow behavior and interactions with protein were quantified via shear viscosity and surface tension for both polysorbates (Figure 2); note that no polysorbate solutions exhibited shear thinning over the range of shear rates examined ($\dot{\gamma} \leq 20\ s^{-1}$). As shown in Figure 2a, no appreciable difference in viscosity is observed between polysorbate 20 and 80 solutions up to 100 mg/mL. Within this range, the solutions have low viscosities that are roughly two-fold that of water or less, and the viscosities do not increase significantly with increasing polysorbate content. Above 100 mg/mL, the viscosity of PS80 increases above that of PS20 and differences in viscosity between the two solutions increase with increasing polysorbate content; these differences are consistent with prior studies on the solution properties of PS20 vs. PS80.[58] Notably, this higher viscosity and poorer solubility of the more hydrophobic PS80 leads to a lower maximum solution concentration vs. that for PS20 (~250 mg/mL vs. ~300 mg/mL, respectively).

While the solution viscosities are nearly independent of polysorbate identity at low concentration, the surface tension of PS20 solutions is always substantially lower than that of PS80 solutions, even at quantities as low as 1 mg/mL (Figure 2b). The stark reduction in surface tension with addition of only 1 mg/mL of each polysorbate is quantitatively consistent with prior works comparing PS20 and PS80 on a mole basis[30,59,60]; note that here, σ is compared on a mass basis and PS20 is slightly smaller than PS80, meaning that additional PS20 molecules can occupy the interface to further lower σ. The higher surface tension in PS80 solutions can also be attributed to differences in polysorbate chemistry. PS80 has a longer hydrophobic tail and thus occupies a larger interfacial area per chain at the air-liquid interface.[59] As a result, a lower density surface layer forms at the interface in PS80 solutions. Additionally, PS20 occupies the interfacial region in substantially higher quantities than PS80, forming a thicker interfacial layer.[59,61,62]

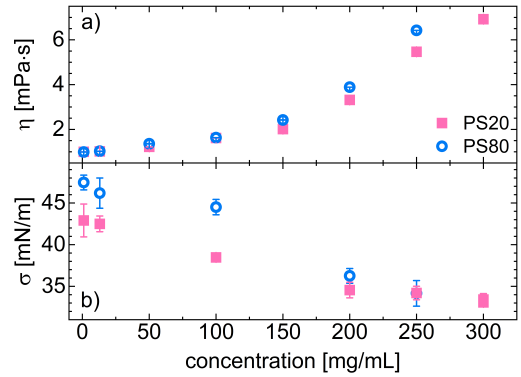

FIGURE 2 a) Newtonian viscosity η and b) surface tension σ of polysorbate 20 and 80 solutions. Solutions did not exhibit shear thinning up to $\dot{\gamma} = 20\ s^{-1}$. At low concentrations, η is equal between polysorbates, whereas σ is ~ 10% lower for PS20 solutions. At high concentrations, η is larger for PS80 solutions, whereas σ plateaus due to saturation at the air-liquid interface and is equal for PS20 and PS80.

DoS measurements on polysorbate 20 and 80 solutions reveal that the capillary thinning behavior of both surfactants is dominated by inertia and surface tension forces (inertiocapillary thinning, Eq. 2), for aqueous concentrations up to 200 mg/mL. Representative radial decay data from PS20 (pink symbols) and PS80 (blue symbols) is shown in Figure 3a; Figure 3b shows the same data on a log-log scaling shifted by t_b to better visualize the power law scaling in different regions during thinning. Note that while Figure 3 shows only a representative trial per solution, all solutions exhibit thinning and breakup behavior that is highly reproducible. This reproducibility is reflected in the narrow distribution and 95% confidence intervals around parameters like the power law index n and breakup time t_b (Table 1; see SI.4 for all raw data). Interestingly, polysorbate concentrations as low as 1 mg/mL significantly increase the breakup time versus that of pure water[23] (t_b = 3.3 ms, Table 1), by ~ 20% and 30% for PS80 and PS20, respectively, due to reduced surface tension forces (Figure 3a, Table 1).

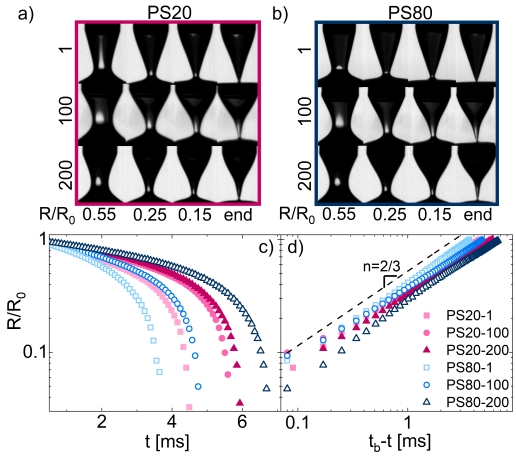

FIGURE 3 Inertiocapillary (IC) thinning images of PS20 (a) vs. PS80 (b) solutions, from 1 mg/mL to 200 mg/mL. Evolution of the liquid bridge radius is shown in time (c) and on a timescale shifted by the breakup time, $t_b - t$ with a constant shifted curve (dotted line) of n=2/3 to show the IC scaling (d) (PS20: pink closed, PS80 blue open shapes).

While IC thinning occurs across polysorbate solutions of ≤200 mg/mL, the average breakup time t_b depends both on polysorbate concentration and identity (Figure 3, Table 1); here, differences in t_b are statistically significant for PS20 vs. PS80 solutions at equivalent concentrations. While the two molecules have similar molecular weights and solution viscosities at 1 mg/mL PS, a 10% increase in breakup time occurs when the surfactant is changed from PS80 (t_b = 3.9 ms, blue □ in Figure 3a) to PS20 (t_b = 4.3 ms, pink ■). While the total polysorbate concentration is small, this result is not surprising given that the differences in thinning behavior are driven by differences in surface tension; at 1 mg/mL, PS80 has a higher surface tension and thus stronger forces driving thinning than PS20 (Figure 2). For the same reasons, the breakup time for PS20 solutions is also ~20% longer than that for PS80 at 100 mg/mL PS (Figure 3, pink • and blue ○, respectively).

Interestingly, the measured breakup time for PS20 exceeds that of PS80 by ~15% at higher concentrations of 200 mg/mL polysorbate, despite the fact that the two solution surface tensions are comparable. Examining the 2D images during thinning provides some insight into these differences (Figure 3a-b). When PS is added at 1 mg/mL, the liquid bridge shape immediately prior to breakup assumes a conical shape as is expected for IC fluids.[46,47] However, despite that the linearized thinning profiles largely follow a $t^{2/3}$ scaling across PS solutions in this concentration regime (Figure 3d, Table 1), the 2D images during thinning become substantially more slender with increasing PS concentration (Figure 3a-b). Similar to prior observations in concentrated P188 solutions,[23] while inertiocapillary behavior describes much of the thinning behavior well, this model is often insufficient to describe the entire thinning process in increasingly concentrated solutions near the concentration border of where flow behaviors such as weak elasticity are observed. This trend becomes apparent when the calculated IC thinning timescale t_R is compared with t_b, which diverge with increasing solution concentration (S1). The narrowing of the filament shape with increasing PS content is particularly evident in PS80-200, which maintains the $t^{2/3}$ scaling at the start of thinning (long $t_b - t$) but deviates near breakup at short $t_b - t$ (Table 1). This increase in power law index near the end of thinning could indicate proximity to either viscocapillary thinning (Eq. 3) or weakly elastic thinning (Eq. 4); however given the low Oh for PS80-200 ($Oh \approx 0.03$), proximity to the latter phenomenon is more likely.

In contrast to prior DoS measurements by Lauser et al.[23] on concentrated P188 (200 mg/mL), here neither PS solution exhibits clear weakly elastic behavior at the equivalent concentration. Instead, the slight increase in slope and liquid bridge shapes observed prior to breakup in PS80-200 are similar to the behavior of P188 at half the aqueous concentration (100 mg/mL).[23] These comparisons suggest that, perhaps as expected, the higher molecular weight of P188 solutions (8.4 kDa vs. ~1 kDa for polysorbates) substantially contributes to the higher elasticity and lower concentration at which weak elasticity is observed in those solutions. Additionally, the comparable P188 solutions consisted primarily of unimers,[23] which may undergo more chain stretching than spherical micelles; prior DoS experiments on spherical poloxamer micelles showed no weakly elastic flow

behavior, albeit at lower solution concentrations.[63]

4.2 IC thinning of OVA/PS solutions

DoS measurements on OVA formulations in the presence of polysorbate excipients reveal that, similar to PS-only solutions, the breakup behavior of OVA/PS solutions is inertiocapillary-driven up to 200 mg/mL total solution concentration (Eq. 2). As expected, the entirety of the thinning behavior for these solutions is well-captured by a $t^{2/3}$ power law scaling (Figure 4d, Table 1), indicating thinning behavior dominated by inertia and surface tension forces. While dilute solutions of 1 mg/mL PS-only showed distinct flow behaviors for PS80 vs. PS20, adding 1 mg/mL PS80 or PS20 to moderately-concentrated 100 mg/mL OVA (denoted OVA100/PS80-1 and OVA100/PS20-1, respectively) leads to capillary thinning behavior that is statistically independent of PS identity (Figure 4), due to the small PS quantity. In 1 mg/mL PS-only solutions, differences in σ between PS80 and PS20 explained the longer breakup times in PS20 solutions. However here, the measured breakup times for OVA100/PS80-1 and OVA100/PS20-1 are identical within statistical certainty, which is perhaps unsurprising given that the surface tensions for the two solutions are also equal (Table 1). The surface tensions for these more concentrated OVA/PS solutions are also lower than that of the 1 mg/mL PS-only solutions, suggesting that OVA migrates to the air-liquid interface to further lower σ. The equal σ between the two OVA solutions with 1 mg/mL PS also suggests that OVA plays a substantial role in lowering the surface tension, given that σ depends on PS identity for 1 mg/mL PS-only solutions. This conclusion is reasonable given that OVA has a mass concentration that is 100-fold larger than that of PS in these solutions, and can thus can effectively compete with PS at the air-liquid interface. Note that while PS identity is unimportant at these low PS contents, adding 1 mg/mL PS to OVA100 does prolong the breakup event relative to 100 mg/mL OVA-only, due to the weaker surface tension forces in PS-containing solutions.

Despite similar timescales for breakup at low polysorbate content, differences in the extensional flow behavior with increasing PS content are well-illustrated by solutions of 100 mg/mL OVA with an additional 100 mg/mL PS80 or PS20 (OVA100/PS80-100 and OVA100/PS20-100, Table 1). Remarkably, the radial decay curves, thinning index n, and breakup times of OVA100 in the presence of 100 mg/mL PS80 are statistically identical to those of OVA100 with 1 mg/mL PS80 – despite that the total macromolecule concentration in solution is twice as large as for OVA100/PS80-100 (Figure 4c-d). Unlike in 200 mg/mL PS80-only solutions, the characteristic IC scaling of $t^{2/3}$ is sufficient to describe the entirety of the thinning behavior for both of these OVA/PS80 solutions (Table 1). Here, σ is statistically identical for OVA100/PS80-1 and OVA100/PS80-100, suggesting that the additional PS80 in the latter case does not lower the surface tension meaningfully. As concentrations of as low as 1 mg/mL PS80 are still far above the PS80 CMC (~0.02 mg/mL[30,36]), formation of PS80 micelles may be favored over further adsorption of PS80 to the air-liquid interface in this concentration regime[18]; PS80 could also replace OVA at the interface but not in sufficiently large quantities to lower the surface tension. As the 2D images during thinning are

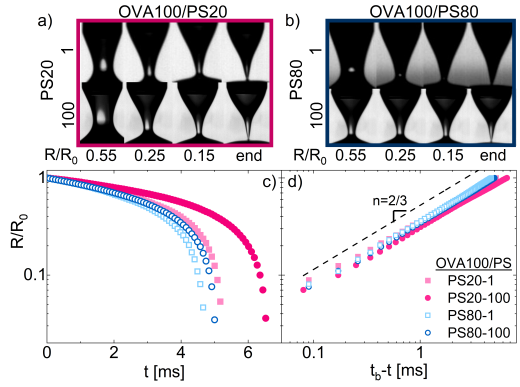

FIGURE 4 Inertiocapillary (IC) thinning behavior of 100 mg/mL OVA with added PS20 or PS80. Evolution of the liquid bridge radius is shown with images for PS20 (a) and PS80 (b), in radius by time data (c) and on a timescale shifted by the breakup time, $t_b - t$ with a constant shifted curve (dotted line) of n=2/3 to show the IC scaling (d)

TABLE 1 Solutions measured via DoS and associated surface tension σ, breakup time t_b, and initial and final thinning indices, n_0 and n. Reported uncertainty is the 95% confidence interval of the parameter value based on fits to all trials (see SI.4 for all raw data). Only n is fit for solutions that are well-described by a single power law index across the entire dataset; however, many reported n and n_0 values overlap, suggesting a single n may be sufficient. * indicates data from Lauser et al.[23], † indicates solution displays weakly elastic thinning in region where n is fit.

sample	total conc. [mg/mL]	σ [mN/m]	t_b [ms]	n_0	n
water*	0	74.1 ± 1.9	3.3 ± 0.1	N/A	0.64 ± 0.02
OVA100*	100	47.5 ± 1.3	4.4 ± 0.3	N/A	0.64 ± 0.02
OVA200*	200	42.1 ± 1.2	6.1 ± 0.4	0.62 ± 0.01	0.64 ± 0.02
PS20-1	1	42.9 ± 1.9	4.3 ± 0.2	N/A	0.67± 0.01
PS20-100	100	38.5 ± 0.5	5.7 ± 0.1	N/A	0.61 ± 0.01
PS20-200	200	34.6 ± 0.9	6.1 ± 0.1	N/A	0.63 ± 0.01
PS20-250	250	34.2 ± 0.8	10.3 ± 0.5	0.59 ± 0.01	0.87 ± 0.08†
PS80-1	1	47.5 ± 0.9	3.9 ± 0.1	N/A	0.68 ± 0.01
PS80-100	100	44.5 ± 0.9	4.4 ± 0.4	N/A	0.63 ± 0.01
PS80-200	200	36.3 ± 0.9	7.1 ± 0.3	0.61 ± 0.01	0.79 ± 0.03
PS80-250	250	34.2 ± 1.5	11.5 ± 1.0	0.44 ± 0.06	0.83 ± 0.04†
OVA100/PS20-1	101	38.1 ± 0.4	5.1 ± 0.2	N/A	0.64 ± 0.01
OVA100/PS20-100	200	36.3 ± 0.5	6.5 ± 0.3	0.65 ± 0.03	0.62 ± 0.01
OVA200/PS20-10	210	36.5 ± 0.4	9.4 ± 0.5	0.54 ± 0.02	0.60 ± 0.03
OVA200/PS20-50	250	35.3 ± 1.1	12.1 ± 0.7	0.51 ± 0.01	0.69 ± 0.03†
OVA200/PS20-100	300	34.3 ± 0.4	16.3 ± 1.4	0.44 ± 0.05	0.84 ± 0.04†
OVA100/PS80-1	101	39.0 ± 0.6	4.9 ± 0.3	N/A	0.64 ± 0.02
OVA100/PS80-100	200	38.1 ± 0.8	5.0 ± 0.1	0.65 ± 0.02	0.64 ± 0.02
OVA200/PS80-10	210	38.7 ± 0.5	10.9 ± 0.1	0.51 ± 0.01	0.64 ± 0.03
OVA200/PS80-50	250	36.3 ± 0.6	12.2 ± 0.6	0.51 ± 0.03	0.71 ± 0.02†
OVA200/PS80-100	300	35.5 ± 1.0	18.4 ± 1.6	0.42 ± 0.07	0.85 ± 0.04†

similar in shape and narrow only slightly with increasing PS80 content (Figure 4b), any possible micelle formation or crowding imparted by the additional PS80 in solution is insufficient to induce weakly elastic behavior.

The surface tension of OVA100/PS80-100 solutions is lower than for PS80-100, suggesting that similar to solutions containing only 1 mg/mL PS, OVA is still present at the interface and meaningfully lowers σ at these higher PS concentrations. The lower surface tension in OVA100/PS80-100 vs. PS80-100 leads to breakup times that are ~15% longer (Table 1). Similar phenomena are observed for PS20-100 and OVA100/PS20-100, where OVA addition in the latter case reduces σ and extends t_b by ~15%.

In contrast to PS80-containing OVA solutions, the breakup behavior for PS20-containing OVA solutions depends on PS20 concentration. Here, OVA100/PS20-100 has a lower surface tension than OVA100/PS20-1, unlike in the analogous PS80-containing formulations where σ is identical. This lower σ in the OVA100/PS20-100 solution leads to a dramatic lengthening in t_b of >25% vs. t_b for OVA100/PS20-1 (Figure 4c-d). Nevertheless, just as in the PS80-containing solutions, the 2D images during thinning are similar in shape and narrow only slightly with additional PS20 content (Figure 4a), suggesting that IC-dominated thinning occurs regardless of additional PS20 adsorbed to the air-liquid interface or potential PS20 micelle formation. Note that while PS20 has a higher CMC than PS80 (~0.06 mg/mL[30,36]), 1 mg/mL PS20 is still far above this value, suggesting a high likelihood of micelle formation given the limited interactions between PS20 and albu-

mins.[31,41] Additionally, PS20 more effectively displaces albumins at air-liquid interfaces than PS80,[61] thus the greater reduction in σ in OVA100 with increasing PS20 vs. PS80 may be due to a greater replacement of OVA by PS20 at the interface. Despite these differences between PS20- and PS80-containing solutions, the 2D images during thinning are nearly identical in shape for analogous PS20- vs PS80-containing solutions (Figure 4a vs. b), again confirming that inertia and surface tension forces dictate the flow behavior in this concentration regime regardless of PS identity.

4.3 Extensional flow of concentrated OVA with increasing polysorbate

While high concentration (200 mg/mL) polysorbate and OVA/PS solutions primarily exhibited inertiocapillary thinning, similar to prior work on OVA/P188 solutions,[23] the increasingly slender liquid bridge shapes immediately prior to breakup suggest that these solutions are in a concentration regime nearing a transition to weakly elastic thinning behavior. Given that injectable therapeutic formulations aim to maximize protein content and minimize excipient content,[17] solutions containing higher protein content (200 mg/mL) with increasing excipient content (10, 50, and 100 mg/mL) were next examined to determine if these formulations continue to thin following IC behavior or if weakly elastic flow behavior instead emerges; representative DoS trials for OVA200 with increasing content of each PS are shown in Figure 5.

While polysorbate-only solutions and OVA/polysorbate solutions at 200 mg/mL exhibit IC thinning behavior, adding PS to OVA200 results in weakly elastic flow behavior in a number of formulations (Figure 5). Remarkably, the flow behavior of concentrated OVA transitions to weakly elastic thinning with as little as 10 mg/mL PS80. As seen in the 2D images immediately prior to breakup (Figure 5a, blue top row), the liquid bridge becomes notably more cylindrical, with an elastic filament observed in the final frame. Notably, while the 2D images in the analogous formulation containing PS20 (OVA200/PS20-10) also become more slender than the traditional cone shape observed in inviscid fluids[46,47] (Figure 3a, top row), clear differences can be seen when these 2D images are compared to those for OVA200/PS80-10. Based on these 2D images and that the slope of the linearized radial decay data does not increase above 2/3 prior to breakup (Figure 5d), this formulation still exhibits primarily IC thinning behavior. The difference in surface tension between these two solutions further supports this conclusion, as OVA200/PS80-10 has a statistically higher surface tension than OVA200/PS20-10 (Table 1). If the extensional flow behavior for both solutions was purely driven by inertia and surface tension, OVA200/PS80-10 would exhibit shorter breakup times than OVA200/PS20-10 due to the higher surface tension forces acting on the liquid bridge. Instead, t_b is substantially higher in OVA200/PS80-10 solutions (Table 1), as can be seen by the vertical lines in Figure 5b-c. Given that the thinning indices at the end of thinning, n, and the beginning of thinning, n_0, are comparable between solutions, the lengthening of the extensional flow response in 200 mg/mL OVA solutions containing 10 mg/mL PS80 vs. those containing PS20 is attributed to the emergence of the weakly elastic flow regime prior to breakup. That the PS80-containing solution transitions to weakly elastic flow behavior at lower concentrations than the PS20-containing solution is perhaps unsurprising given that PS80-200 is closer to the onset of this transition than PS20-200.

The emergence of weakly elastic flow behavior in OVA200/PS80-10 is also apparent when the 2D images and breakup times are compared to those for the IC-dominated OVA100/PS80-100 solutions. While these solutions have nearly equal total solution concentrations (~200 mg/mL), the filament immediately prior to breakup for OVA200/PS80-10 is slender and cylindrical whereas OVA100/PS80-100 maintains a conical shape which only slightly narrows in comparison to lower concentration solutions (Figure 5a vs. Figure 4b). These two solutions have identical surface tensions (Table 1), yet the breakup times for OVA200/PS80-10 are over double that of OVA100/PS80-100, clearly indicating that IC thinning alone is insufficient to fully describe the ex-

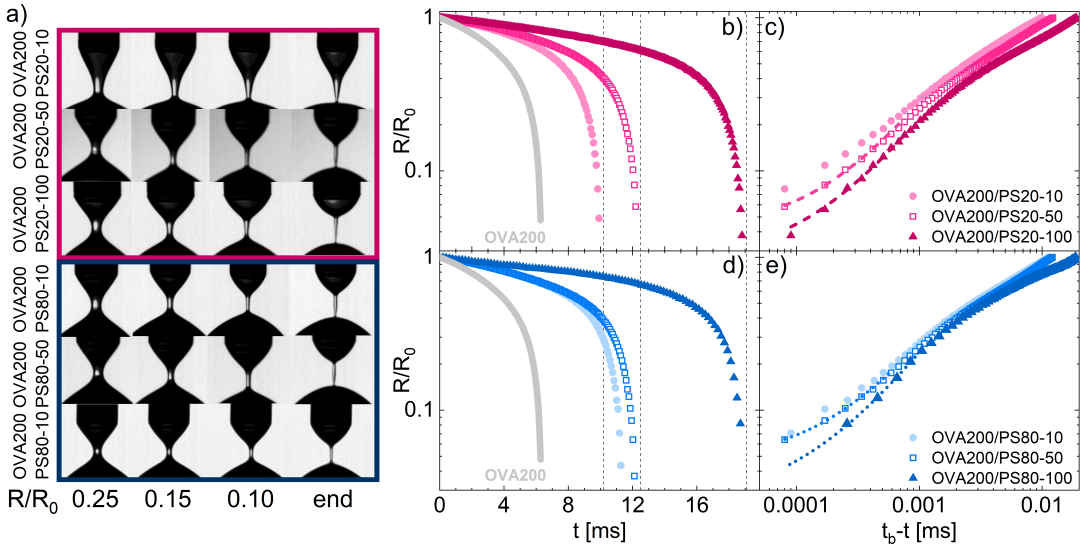

FIGURE 5 (a) 2D images of the thinning behavior of OVA200 solutions with added PS20 and PS80 (10, 50, 100 mg/mL). Evolution of the liquid bridge radius is shown in time for (b) PS20 and (d) PS80, and on a timescale shifted by $t_b - t$ in (c) for PS20 and (e) for PS80. In (b,d), dotted lines after each t_b are included for visual aid to compare analogous t_b; OVA200 is shown in gray for reference. In (c,e), dotted lines are fits to the semi-empirical Anna-McKinley model (Eq. 4).[53]

tensional behavior. Interestingly, while OVA200/PS20-10 does not exhibit a clear transition to weakly elastic behavior, its breakup time is still prolonged by ~40% in comparison to OVA100/PS20-100 despite equal σ, just as in the analogous PS80-containing solutions. This behavior is attributed to the high solution OVA content, which has previously been shown to slow the initial thinning process characterized by index n_0[23] (Table 1), which may reflect the particle-like nature of OVA.[23,52]

With increasing polysorbate concentration (≥50 mg/mL), differences in extensional flow behavior between solutions containing PS20 vs. PS80 virtually disappear, as suggested by the nearly identical 2D snapshots during thinning when solutions containing PS20 are compared to those containing PS80 (Figure 5a). This similarity in thinning behavior leads to breakup times that are identical within statistical certainty for analogous PS20- and PS80-containing solutions (see vertical lines in Figure 5b-c, Table 1). The 2D images prior to breakup appear similar between OVA solutions containing either 10 mg/mL or 50 mg/mL PS80, suggesting that both solutions exhibit weakly elastic extensional flow behavior. Conversely, the filament becomes notably more slender and cylindrical when OVA200 solutions containing 50 mg/mL PS20 are compared to those containing 10 mg/mL PS20 (Figure 5a), suggesting that by 50 mg/mL PS20, the solution has transitioned from IC-dominated to weakly elastic thinning immediately prior to breakup. Similar thinning shapes are observed at the highest PS content for both PS20 and PS80, confirming that weakly elastic thinning persists with increasing PS content.

In these crowded solutions, the surface tensions have reached a near plateau value with increasing concentration, and are statistically identical between analogous solutions containing OVA with PS80 or PS20 (Table 1). This finding is unsurprising given that at high macromolecule concentrations, the air-water interface will become saturated; a similar plateau in the surface tension is observed with increasing concentration in PS-only solutions (Figure 2). However similar to observations in OVA/P188 solutions,[23] OVA reduces the surface ten-

sion less effectively than PS on a per mass basis (Table 1); for example, at 200 mg/mL concentration, the surface tension is ~20% lower in PS solutions vs. OVA solutions. Thus while distinct differences in σ are observed based on PS identity in OVA200/PS-10 solutions due to low PS content, further increasing PS content largely eliminates these differences, thereby removing the major mechanism driving distinct IC breakup timescales at lower solution concentrations.

The weakly elastic flow behavior observed in OVA solutions with ≥50 mg/mL PS is fit with the semi-empirical Anna-McKinley model to extract rheological parameters (Eq. 4), confirming that no statistically significant differences in extensional flow behavior are observed based on PS identity in this concentration regime (Table 2). Here, a distinct transition to elastocapillary thinning (Eq. 5) is never observed, justifying the use of Eq. 4; note that due to a scarcity of points and large number of fitting parameters in Eq. 4, OVA200/PS80-10 trials were not fit to avoid over-fitting. Both OVA200 solutions containing 100 mg/mL PS exhibit extensional relaxation times of $\lambda_E \approx 4$ ms; the corresponding infinite extensional viscosities and elastic filament lifetimes are also statistically identical: $\eta_E^\infty \sim 0.16$ Pa·s and $t_E \sim 1.4$ ms, respectively. As expected, OVA200 formulations containing less polysorbate (50 mg/mL) exhibit shorter λ_E and t_E than solutions containing 100 mg/mL PS (Table 2). However just as in their higher PS-content counterparts, the extracted rheological parameters are independent of PS identity for OVA200/PS-50 formulations.

The conclusion that the thinning behavior is independent of PS identity for ultra-high concentration (≥250 mg/mL) OVA/PS solutions is supported by DoS measurements on 250 mg/mL PS solutions, which are also indistinguishable based on PS identity (Figure 6). Increasing the concentration from 200 mg/mL to 250 mg/mL for both polysorbates results in a transition from IC-dominated to weakly elastic thinning immediately prior to breakup, where t_b also increases by >60% (Table 1). As shown in Figure 6, the 2D images, radial decay profiles, and linearized decay profiles are all nearly identical between 250 mg/mL PS20 and PS80; unsurprisingly, extracted rheological parameters using Eq. 4 are also identical (Table 2). While differences in flow behavior based on PS identity at total concentrations below 200 mg/mL are primarily driven by surface tension differences, here the solutions are sufficiently concentrated such that σ is identical between the two polysorbates (Figure 2, Table 1). Thus without surface tension differences to drive changes in extensional flow behavior, these crowded PS solutions exhibit similar thinning behaviors due to their identical concentration in solution; the marginally higher shear viscosity and slightly larger micelle size[40] for PS80 solutions is insufficient to change the extensional flow behavior appreciably.

TABLE 2 Extensional flow parameters extracted using the semi-empirical Anna-McKinley model for weakly elastic flow behavior (Eq. 4). No statistically significant differences in λ_E, η_E^∞, or t_E are observed for analogous solutions with either PS20 or PS80; however, statistically significant differences in λ_E and t_E are observed between each formulation type. Reported uncertainties are the 95% confidence intervals around mean values from multiple trials.

sample	total conc. [mg/mL]	λ_E [ms]	η_E^∞ [Pa· s]	t_E [ms]
OVA200/PS20-50	250	2.5 ± 0.2	0.15 ± 0.01	0.5 ± 0.1
OVA200/PS80-50	250	2.6 ± 0.1	0.15 ± 0.01	0.6 ± 0.1
OVA200/PS20-100	300	4.0 ± 0.1	0.16 ± 0.01	1.3 ± 0.1
OVA200/PS80-100	300	4.1 ± 0.1	0.17 ± 0.02	1.5 ± 0.1
PS20-250	250	2.9 ± 0.2	0.14 ± 0.01	0.9 ± 0.1
PS80-250	250	3.0 ± 0.2	0.14 ± 0.02	0.8 ± 0.1

The magnitude of the rheological parameters extracted from fits to Eq. 4 across high concentration solutions also supports the prior conclusion that this transition to weakly elastic thinning depends on both PS content and total solution concentration. At equal solution concentration (250 mg/mL), the extensional relaxation time and elastic filament lifetime are longer for PS-only solutions than for OVA200/PS-50 solutions (Table 2); this finding suggests that polysorbate contributes more to the weakly elastic flow behavior than OVA, as expected given that OVA-only solutions never show weakly elastic thinning. However, OVA contributes to this flow phenomenon by increasing the total concen-

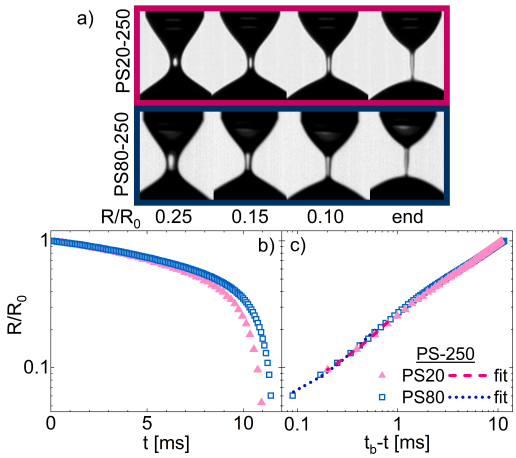

FIGURE 6 (a) Images of weakly elastic thinning behavior of 250 mg/mL PS20 and PS80. (b) Evolution of the liquid bridge radius is shown in time, and (c) on a shifted timescale, $t_b - t$. Fits to Eq. 4 are shown in dashed lines. As can be deduced by the images and radial decay profiles, no statistically significant difference in extensional flow behavior is observed between these two high PS content solutions.

tration, which also critically impacts the observed elasticity. For example, higher concentration OVA200/PS-100 solutions (300 mg/mL) have larger λ_E and t_E than 250 mg/mL PS-only solutions, and the increase in λ_E is substantially more when the solution concentration is increased (OVA200/PS-100 vs. PS250) vs. when the PS content is increased at constant total concentration (PS250 vs. OVA200/PS-50).

4.4 Dependence of extensional flow behavior on formulation parameters

The dominant flow behavior in OVA/PS solutions depends on total solution concentration, which dictates the relative importance of PS identity vs. quantity. At and below 200 mg/mL, thinning behavior is driven by inertial and surface tension forces (IC thinning) in OVA-only, PS-only, and OVA/PS solutions. In all cases where weakly elastic thinning is observed, the presence of both OVA and polysorbate are required; note that both OVA200 and OVA300 exhibit IC thinning behavior[23]. This conclusion is similar to that in prior work on OVA/P188 solutions; however OVA200 was examined only with high P188 content (100 mg/mL).[23] That weakly elastic thinning behavior in extensional flow emerges in ultra-concentrated solutions at substantially lower excipient concentrations than previously observed underscores the importance of selecting proper excipients – and of assessing both shear and extensional flow properties, as the shear rheology for PS-only solutions showed Newtonian behavior over the measured shear rate range.

Above 200 mg/mL total concentration, the observed flow behavior is a function of solution composition and relative quantity of PS to OVA. The distinct behavior observed between PS80- and PS20-containing OVA formulations with 10 mg/mL PS suggests that the polysorbate identity impacts the observed flow behavior in high OVA content solutions when PS is present in small amounts. As OVA-only solutions at 300 mg/mL exhibit only IC thinning, this weakly elastic flow behavior cannot be explained entirely by the small increase in solution concentration to 210 mg/mL. However, the emergence of weakly elastic flow behavior with the addition of only an additional 10 mg/mL material to the solution is unsurprising given prior work showing an exponential rise in protein solution shear viscosity can occur with increasing concentration in ultra-high concentration therapeutics.[7,14] These large changes in shear viscosity with small increases in macromolecule solution concentration often occur due to changing interactions between components in solution.

In the 200 mg/mL OVA solutions with 10 mg/mL PS, the differing interactions that PS20 vs. PS80 have with OVA could influence the appearance of the weakly elastic behavior, among other factors. We note that while the nature of DoS measurements leads solutions to experience non-uniform extension rates, these solutions all experience similar extension rate profiles (SI.2). While PS20 and PS80 solutions have identical zero-shear viscosities at low concentrations (Figure 2), at high polysorbate content, PS80 has a higher viscosity than PS20. While the zero-shear viscosity cannot be measured accurately in the protein-containing solutions in a conventional rheometer, the high solution concentra-

tion here could also lead to a higher zero-shear viscosity for OVA200/PS80-10 than for OVA200/PS20-10. If the zero-shear viscosity became sufficiently large such that viscous forces became important in the thinning process ($Oh > 1$, Eq. 1), the radial decay would also be expected to slow for the OVA200/PS80-10 solution. However, given that the 250 mg/mL PS solutions exhibit identical thinning behavior despite differences in zero-shear viscosity (Figure 2), any viscosity differences impacting the extensional flow behavior are likely instead due to OVA/PS interactions. Additionally, as greater surface tension would suggest a faster – not longer – breakup time for OVA200/PS80-10 vs. OVA200/PS20-10, the observed differences in extensional flow behavior are hypothesized to be largely due to differing interactions between OVA and each polysorbate; potential differences in elasticity originating from the PS itself could also contribute, given that PS80-200 appeared closer to the onset of weak elasticity than PS20-200. Thus consistent with prior work showing that PS20 and PS80 in low quantities impact the shear viscosity of ultra-concentrated proteins differently,[14] PS identity appears to critically impact extensional flow metrics dictating injectability in ultra-concentrated proteins when added at low concentrations, as is current practice.

That the 200 mg/mL OVA solutions thin nearly identically in the presence of either polysorbate once the PS concentration is at or above 50 mg/mL suggests that the flow behavior in this concentration regime is largely dictated by solution concentration and excluded volume effects rather than the PS identity. This hypothesis is reasonable given that the large number of prior works on PS20 vs. PS80 solution behaviors concluding that differences in PS-albumin interactions between the two polysorbates are small.[31,37,41] In the limit of a small PS:OVA ratio, the polysorbate identity and impact on surface tension and interactions with OVA are more likely to alter the flow properties vs. the regime in which both PS and OVA content are high. Additionally, differences in extensional flow behavior between the OVA/PS solutions at lower OVA content (100 mg/mL) were largely driven by differences in surface tension; whereas in analogous higher concentration formulations, no statistically significant differences in surface tension are observed.

While current formulations employ low concentrations of nonionic surfactant excipients,[17] numerous studies have shown that increasing the excipient content may be required for stability and optimal shear viscosity in ultra-high concentration formulations.[14,33] While selecting PS20 over PS80 may be preferable for improving injectability at low PS content like in OVA200/PS-10, in these high excipient content regimes, differentiating between PS identities may not be necessary during formulation. Instead, a focus on reducing weakly elastic behavior – which could detrimentally impact protein structure and formulation injectability but will likely occur at these higher surfactant contents – should be pursued. Finally, we note that this excipient selection criteria is solely based on extensional flow stability: excipient-dependent interactions at rest or in shear flows can lead to degradation or other stability loss over long timescales, and must also be carefully considered.[16–18]

5 Conclusions

While both polysorbates have similar molecular weights and headgroups, the extensional flow behavior of ovalbumin-polysorbate solutions greatly depends on polysorbate identity in two regimes: when the total solution concentration is $\leq$200 mg/mL or in ultra-concentrated OVA when the PS:OVA ratio is small. In less concentrated solutions exhibiting primarily inertiocapillary-driven thinning, associated breakup times are longer in PS20-containing solutions, due to its higher efficiency in reducing the solution surface tension. Similar to prior work on polymeric excipient-protein solutions, undesirable elasticity is still observed in some high-concentration OVA/excipient formulations. In comparison to higher molecular weight P188 excipients, polysorbate-only solutions require substantially higher concentrations to transition to weakly elastic flow behavior; this difference is attributed to the more compact PS structure and the presence of micelles in solution vs. P188 unimers that can stretch under ex-

tension.

Evidence from polysorbate-only solutions and from concentrated OVA with low PS content suggests that PS80-containing solutions transition to weakly elastic thinning behaviors at lower concentrations than those containing PS20. Notably, a transition to weakly elastic flow behavior can be observed with addition of as little as 10 mg/mL PS80 to concentrated OVA (200 mg/mL); in the analogous PS20 formulation, inertiocapillary thinning is instead observed. Thus in this low PS:OVA ratio regime, PS identity can influence the observed flow regime. However, beyond a critical PS content, the extensional flow behavior in PS-only and OVA/PS solutions becomes indistinguishable based on PS identity. In agreement with prior stability studies, the reported extensional flow behaviors suggest that the protective interactions between proteins and excipients in dilute solution may be mitigated in more crowded solution environments, motivating the design and development of novel excipients for ultra-high concentration formulations. Additionally, the stark contrast in the observed shear vs. extensional flow behavior in protein-excipient solutions demonstrates the need to evaluate formulation stability with respect to both shear and extensional flow properties. The dripping-onto-substrate methodology thus provides one straightforward route to assess the extensional rheology and injectability of protein solutions containing new excipients specifically formulated for flow stability.

Acknowledgements

This material is based upon work supported by the National Science Foundation Graduate Research Fellowship under Grant No. CON-75851, project 00074041. Any opinions, findings, and conclusions or recommendations expressed in this material are those of the author(s) and do not necessarily reflect the views of the National Science Foundation. The authors thank the Anton Paar VIP program for the shear rheometer used in this work.

Conflict of Interest

The authors declare no competing interests.

Supporting Information

Supporting information for this article contains chemical and protein structures, and all raw DoS data.

Notes and references

[1] Joseph L Mann, Caitlin L Maikawa, Anton AA Smith, Abigail K Grosskopf, Sam W Baker, Gillie A Roth, Catherine M Meis, Emily C Gale, Celine S Liong, Santiago Correa, et al. An ultrafast insulin formulation enabled by high-throughput screening of engineered polymeric excipients. *Science Trans. Med.*, 12(550): 6676, 2020.

[2] Laura M Marquardt, Vanessa M Doulames, Alice T Wang, Karen Dubbin, Riley A Suhar, Michael J Kratochvil, Zachary A Medress, Giles W Plant, and Sarah C Heilshorn. Designer, injectable gels to prevent transplanted schwann cell loss during spinal cord injury therapy. *Science Adv.*, 6(14):eaaz1039, 2020.

[3] Patrick M Buck, Anuj Chaudhri, Sandeep Kumar, and Satish K Singh. Highly viscous antibody solutions are a consequence of network formation caused by domain–domain electrostatic complementarities: Insights from coarse-grained simulations. *Mol. Pharm.*, 12(1):127–139, 2015.

[4] Samir Mitragotri, Paul A Burke, and Robert Langer. Overcoming the challenges in administering biopharmaceuticals: formulation and delivery strategies. *Nat. Rev. Drug Discov.*, 13(9):655–672, 2014.

[5] Jun Liu, Mary DH Nguyen, James D Andya, and Steven J Shire. Reversible self-association increases the viscosity of a concentrated monoclonal antibody in aqueous solution. *J. Pharm. Sci.*, 94(9):1928–1940, 2005.

[6] Steven J Shire, Zahra Shahrokh, and JUN Liu. Challenges in the development of high protein concentration formulations. *J. Pharm. Sci.*, 93(6):1390–1402, 2004.

[7] Brian D Connolly, Chris Petry, Sandeep Yadav, Barthélemy Demeule, Natalie Ciaccio, Jamie MR Moore, Steven J Shire, and Yatin R Gokarn. Weak

interactions govern the viscosity of concentrated antibody solutions: high-throughput analysis using the diffusion interaction parameter. *Biophys. J.*, 103(1):69–78, 2012.

[8] Lois Jovanovic-Peterson, Suzanne Sparks, Jerry P Palmer, and Charles M Peterson. Jet-injected insulin is associated with decreased antibody production and postprandial glucose variability when compared with needle-injected insulin in gestational diabetic women. *Diabetes Care*, 16(11):1479–1484, 1993.

[9] Nitin Rathore, Pratik Pranay, Joseph Bernacki, Bruce Eu, Wenchang Ji, and Ed Walls. Characterization of protein rheology and delivery forces for combination products. *J. Pharm. Sci.*, 101(12):4472–4480, 2012.

[10] Maria A Miller, Joshua D Engstrom, Baltej S Ludher, and Keith P Johnston. Low viscosity highly concentrated injectable nonaqueous suspensions of lysozyme microparticles. *Langmuir*, 26(2):1067–1074, 2009.

[11] Jan Jezek, Martin Rides, Barry Derham, Jonathan Moore, Elenora Cerasoli, Robert Simler, and Bernardo Perez-Ramirez. Viscosity of concentrated therapeutic protein compositions. *Adv. Drug Delivery Rev.*, 63(13): 1107–1117, 2011.

[12] Zhenhuan Zhang and Yun Liu. Recent progresses of understanding the viscosity of concentrated protein solutions. *Curr. Opin. Chem. Eng.*, 16:48–55, 2017.

[13] Danika Rodrigues, Laura M Tanenbaum, Renuka Thirumangalathu, Sandeep Somani, Kai Zhang, Vineet Kumar, Ketan Amin, and Santosh V Thakkar. Product-specific impact of viscosity modulating formulation excipients during ultra-high concentration biotherapeutics drug product development. *J. Pharm. Sci.*, 110(3): 1077–1082, 2021.

[14] Neal Whitaker, Jian Xiong, Samantha E Pace, Vineet Kumar, C Russell Middaugh, Sangeeta B Joshi, and David B Volkin. A formulation development approach to identify and select stable ultra–high-concentration monoclonal antibody formulations with reduced viscosities. *J. Pharm. Sci.*, 106(11):3230–3241, 2017.

[15] Sandeep Yadav, Steven J Shire, and Devendra S Kalonia. Factors affecting the viscosity in high concentration solutions of different monoclonal antibodies. *J. Pharm. Sci.*, 99(12):4812–4829, 2010.

[16] Tim J Kamerzell, Reza Esfandiary, Sangeeta B Joshi, C Russell Middaugh, and David B Volkin. Protein–excipient interactions: Mechanisms and biophysical characterization applied to protein formulation development. *Adv. Drug Deliv. Rev.*, 63(13):1118–1159, 2011.

[17] Tarik A Khan, Hanns-Christian Mahler, and Ravuri SK Kishore. Key interactions of surfactants in therapeutic protein formulations: a review. *Eur. J. Pharm. Biopharm.*, 97:60–67, 2015.

[18] Hyo Jin Lee, Arnold McAuley, Karl F Schilke, and Joseph McGuire. Molecular origins of surfactant-mediated stabilization of protein drugs. *Adv. Drug Delivery Rev.*, 63(13):1160–1171, 2011.

[19] Samiul Amin, Gregory V Barnett, Jai A Pathak, Christopher J Roberts, and Prasad S Sarangapani. Protein aggregation, particle formation, characterization & rheology. *Curr. Opin. Colloid Interface Sci.*, 19(5):438–449, 2014.

[20] Innocent B Bekard, Peter Asimakis, Joseph Bertolini, and Dave E Dunstan. The effects of shear flow on protein structure and function. *Biopolymers*, 95(11): 733–745, 2011.

[21] Maria Monica Castellanos, Jai A Pathak, and Ralph H Colby. Both protein adsorption and aggregation contribute to shear yielding and viscosity increase in protein solutions. *Soft Matter*, 10(1):122–131, 2014.

[22] Jeffrey S Horner, Antony N Beris, Donna S Woulfe, and Norman J Wagner. Effects of ex vivo aging and storage temperature on blood viscosity. *Clin. Hemorheol. Microcirc.*, 70(2):155–172, 2018.

[23] Kathleen T Lauser, Amy L Rueter, and Michelle A Calabrese. Small-volume extensional rheology of concentrated protein and protein-excipient solutions. *Soft Matter*, 17(42):9624–9635, 2021.

[24] M Brust, C Schaefer, R Doerr, L Pan, M Garcia, PE Arratia, and C Wagner. Rheology of human blood plasma: Viscoelastic versus newtonian behavior. *Phys. Rev. Lett.*, 110(7):078305, 2013.

[25] Alfredo Lanzaro. A microfluidic approach to studying the injection flow of concentrated albumin solutions. *SN Appl. Sci.*, 3(9):1–10, 2021.

[26] S Rammensee, U Slotta, T Scheibel, and AR Bausch. Assembly mechanism of recombinant spider silk proteins. *Proc. Natl. Acad. Sci.*, 105(18):6590–6595, 2008.

[27] John Dobson, Amit Kumar, Leon F Willis, Roman Tuma, Daniel R Higazi, Richard Turner, David C Lowe, Alison E Ashcroft, Sheena E Radford, Nikil Kapur, and David J. Brockwell. Inducing protein aggregation by extensional flow. *Proc. Natl. Acad. Sci.*, 114(18):4673–4678, 2017.

[28] Leon F Willis, Amit Kumar, John Dobson, Nicholas J Bond, David Lowe, Richard Turner, Sheena E Radford, Nikil Kapur, and David J Brockwell. Using extensional flow to reveal diverse aggregation landscapes for three igg1 molecules. *Biotechnol. Bioeng.*, 115(5): 1216–1225, 2018.

[29] H Hosseini, A Rangchian, ML Prins, CC Giza, JW Ruberti, and HP Kavehpour. Probing flow-induced biomolecular interactions with micro-extensional rheology: Tau protein aggregation. *J. Biomech. Eng.*, 142 (3):034501, 2020.

[30] Patrick Garidel, Michaela Blech, Julia Buske, and Alfred Blume. Surface tension and self-association properties of aqueous polysorbate 20 hp and 80 hp solutions: insights into protein stabilisation mechanisms. *J. Pharm. Innov.*, pages 1–9, 2020.

[31] Claudia Hoffmann, Alfred Blume, Inge Miller, and Patrick Garidel. Insights into protein–polysorbate interactions analysed by means of isothermal titration and differential scanning calorimetry. *Eur. Biophys. J.*, 38(5):557–568, 2009.

[32] R.R. Niño and J.M.R. Patino. Surface tension of bovine serum albumin and tween 20 at the air–aqueous interface. *J. Am. Oil Chem. Soc.*, 75(10):1241–1248, 1998.

[33] Akhilesh Bhambhani, Julian M Kissmann, Sangeeta B Joshi, David B Volkin, Ramesh S Kashi, and C Russell Middaugh. Formulation design and high-throughput excipient selection based on structural integrity and conformational stability of dilute and highly concentrated igg1 monoclonal antibody solutions. *J. Pharm. Sci.*, 101(3):1120–1135, 2012.

[34] Paschalis Alexandridis, Josef F Holzwarth, and T Alan Hatton. Micellization of poly (ethylene oxide)-poly (propylene oxide)-poly (ethylene oxide) triblock copolymers in aqueous solutions: thermodynamics of copolymer association. *Macromolecules*, 27(9):2414–2425, 1994.

[35] Priya Sellaturay, Padmalal Gurugama, Verah Harper, Tom Dymond, Pamela Ewan, and Shuaib Nasser. The polysorbate containing astrazeneca covid-19 vaccine is tolerated by polyethylene glycol (peg) allergic patients. *Clinical & Experimental Allergy*, 52(1):12–17, 2022.

[36] Lucy SC Wan and Philip FS Lee. Cmc of polysorbates. *J. Pharm. Sci.*, 63(1):136–137, 1974.

[37] Miriam Ruiz-Peña, Reinier Oropesa-Nuñez, Tirso Pons, Sonia Renaux W. Louro, and Aurora Pérez-Gramatges. Physico-chemical studies of molecular interactions between non-ionic surfactants and bovine serum albumin. *Colloids Surf. B: Biointerfaces*, 75:282–289, 2010.

[38] Jannatun Nayem, Zhenhuan Zhang, Anthony Tomlinson, Isidro E Zarraga, Norman J Wagner, and Yun Liu. Micellar morphology of polysorbate 20 and 80 and their ester fractions in solution via small-angle neutron scattering. *J. Pharm. Sci.*, 109(4):1498–1508, 2020.

[39] Jeffrey Penfold, Robert K Thomas, Peixun X Li, Jordan T Petkov, Ian Tucker, John RP Webster, and Ann E Terry. Adsorption at air–water and oil–water interfaces and self-assembly in aqueous solution of ethoxylated polysorbate nonionic surfactants. *Langmuir*, 31 (10):3003–3011, 2015.

[40] Subhash C Bhattacharya, Haritaran Das, and Satya P Moulik. Effects of solvent and micellar enviroment on the spectroscopic behavior of the dye safranine t. *J. Photochem. Photobiol. A: Chem.*, 79(1-2):109–114, 1994.

[41] Patrick Garidel, Claudia Hoffmann, and Alfred Blume. A thermodynamic analysis of the binding interaction between polysorbate 20 and 80 with human serum albumins and immunoglobulins: a contribution to understand colloidal protein stabilisation. *Biophys. Chem.*, 143(1-2):70–78, 2009.

[42] Ananyo A Bhattacharya, Tim Grüne, and Stephen Curry. Crystallographic analysis reveals common modes of binding of medium and long-chain fatty acids to human serum albumin. *J. Mol. Biol.*, 303(5): 721–732, 2000.

[43] G. H. McKinley. Visco-elasto-capillary thinning and break-up of complex fluids. *Rheology Reviews*, 05-P-04:1–50, 2005.

[44] Jelena Dinic, Yiran Zhang, Leidy Nallely Jimenez, and Vivek Sharma. Extensional relaxation times of dilute, aqueous polymer solutions. *ACS Macro Lett.*, 4(7):804–808, 2015.

[45] Leidy Nallely Jimenez, Jelena Dinic, Nikhila Parsi, and Vivek Sharma. Extensional relaxation time, pinch-off dynamics, and printability of semidilute polyelectrolyte solutions. *Macromolecules*, 51(14):5191–5208, 2018.

[46] Richard F Day, E John Hinch, and John R Lister. Self-similar capillary pinchoff of an inviscid fluid. *Phys. Rev. Lett.*, 80(4):704, 1998.

[47] J Rafa Castrejón-Pita, Alfonso A Castrejón-Pita, E John Hinch, John R Lister, and Ian M Hutchings. Self-similar breakup of near-inviscid liquids. *Phys. Rev. E*, 86 (1):015301, 2012.

[48] D Howell Peregrine, G Shoker, and A Symon. The bifurcation of liquid bridges. *J. Fluid Mech.*, 212:25–39, 1990.

[49] M. Rosello, S Sur, B Barbet, and J.P. Rothstein. Dripping-onto-substrate capillary breakup extensional rheometry of low-viscosity printing inks. *J. Non-Newton Fluid*, 2019.

[50] Laura Campo-Deano and Christian Clasen. The slow retraction method (srm) for the determination of ultra-short relaxation times in capillary breakup extensional rheometry experiments. *J. Nonnewton. Fluid Mech.*, 165(23-24):1688–1699, 2010.

[51] Demetrios T Papageorgiou. Analytical description of the breakup of liquid jets. *J. Fluid Mech.*, 301:109–132, 1995.

[52] Jelena Dinic, Leidy Nallely Jimenez, and Vivek Sharma. Pinch-off dynamics and dripping-onto-substrate (DoS) rheometry of complex fluids. *Lab Chip*, 17(3):460–473, 2017.

[53] Shelley L Anna and Gareth H McKinley. Elasto-capillary thinning and breakup of model elastic liquids. *J. Rheol.*, 45(1):115–138, 2001.

[54] Jelena Dinic and Vivek Sharma. Power laws dominate shear and extensional rheology response and capillarity-driven pinching dynamics of entangled hydroxyethyl cellulose (hec) solutions. *Macromolecules* 53(9):3424–3437, 2020.

[55] C. E. Sing and A. Alexander-Katz. Elongational flow induces the unfolding of von Willebrand factor at physiological flow rates. *Biophys. J.*, 98(9):L35–L37, 2010.

[56] A. Mogne Daeer, A. Pendentdrop: An imagej plugin to measure the surface tension from an image of a pendent drop. *J. Open Res. Softw.*, 4:e3, 2016.

[57] NB Vargaftik, BN Volkov, and LD Voljak. International tables of the surface tension of water. *J. Phys. Chem. Ref. Data*, 12(3):817–820, 1983.

[58] AB Mandal, Syamasri Gupta, and SP Moulik. Characterisation of tween 20 & tween 80 micelles in aqueous medium from transport studies. *Indian J. Chem.*, 24A: 670–673, 1985.

[59] Agata Bąk and Wioletta Podgórska. Interfacial and surface tensions of toluene/water and air/water systems with nonionic surfactants tween 20 and tween 80. *Colloids Surf. A: Physicochem. Eng. Asp.*, 504:414–425, 2016.

[60] Sayantan Samanta and Pallab Ghosh. Coalescence of bubbles and stability of foams in aqueous solutions of tween surfactants. *Chem. Eng. Res. Des.*, 89(11):2344–2355, 2011.

[61] Martin Rabe, Andreas Kerth, Alfred Blume, and Patrick Garidel. Albumin displacement at the air–water interface by tween (polysorbate) surfactants. *Eur. Biophys. J.*, 49(7):533–547, 2020.

[62] Graham H Cross, Andrew Reeves, Stuart Brand, Marcus J Swann, Louise L Peel, Neville J Freeman, and Jian R Lu. The metrics of surface adsorbed small molecules on the young's fringe dual-slab waveguide interferometer. *J. Phys. D: Appl. Phys.*, 37(1):74, 2003.

[63] Diana Y Zhang and Michelle A Calabrese. Temperature-controlled dripping-onto-substrate (dos) extensional rheometry of polymer micelle solutions. *Soft Matter*, 2022. URL `http://www.doi.org/10.1039/d2sm00377e`.

6 graphical abstract